Michigan Math. J. 55 (2007)

The Space of Doubly Periodic Minimal Tori with Parallel Ends: Standard Examples

M. MAGDALENA RODRÍGUEZ

1. Introduction

Scherk [10] presented in 1835 the first properly embedded minimal surface in $\mathbb{R}^3$ that was invariant by two linearly independent translations; we will shorten by saying a *doubly periodic minimal surface*. (Unless explicitly mentioned, all surfaces in this paper are presumed to be connected and orientable.) This surface is known as *Scherk's first surface,* and it fits naturally into a 1-parameter family $\mathcal{F} = \{F_\theta\}_\theta$ of examples known as doubly periodic Scherk minimal surfaces. In the quotient by its more refined period lattice (i.e., the period lattice generated by its shortest period vectors), each F_θ has genus 0 and four asymptotically flat annular ends: two top and two bottom ones, provided that the period lattice is horizontal. This kind of annular end is called a *Scherk-type end*. The parameter θ in this family $\mathcal{F}$ is the angle between top and bottom ends of F_θ. We can clearly consider the quotient of these F_θ by a less refined period lattice to have two top and $2k$ bottom ends for any natural k, keeping genus 0 in the quotient. Lazard-Holly and Meeks [5] proved that these are the only possible examples in this setting; that is, if the quotient of a doubly periodic minimal surface $M \subset \mathbb{R}^3$ has genus 0, then M must be a doubly periodic Scherk minimal surface up to translations, rotations, and homotheties. Moreover, the angle map $\theta\colon \mathcal{F} \to (0,\pi)$ is a diffeomorphism. Hence the moduli space of properly embedded minimal surfaces with genus 0 in $\mathbb{T}\times\mathbb{R}$, $\mathbb{T}$ a flat torus, is diffeomorphic to $(0,\pi)$ after identifying by rotations, translations, and homotheties.

In 1988, Karcher [3] defined another 1-parameter family of doubly periodic minimal surfaces, called *toroidal half-plane layers,* with genus 1 and four Scherk-type parallel ends in its smallest fundamental domain (these examples will be denoted as $M_{\theta,0,0}$ in Section 2). Furthermore, he exposed two distinct 1-parameter deformations of each toroidal half-plane layer and so obtained other doubly periodic minimal tori with parallel ends (denoted as $M_{\theta,\alpha,0}$ and $M_{\theta,0,\beta}$, with $\beta < \theta$, in Section 2). We generalize these Karcher's examples in Section 2 by obtaining a 3-parameter family.

THEOREM 1. *There exists a* 3*-parameter family* $\mathcal{K} = \{M_{\theta,\alpha,\beta}\}_{\theta,\alpha,\beta}$ *of properly embedded doubly periodic minimal surfaces with genus* 1 *and four parallel ends*

Received May 3, 2005. Revision received October 17, 2006.
Research partially supported by MEC/FEDER Grant no. MTM2004-02746.

in the quotient by their more refined period lattices. This family $\mathcal{K}$ can be endowed with a natural structure of a real-analytic 3-dimensional manifold with the topology of the uniform convergence on compact sets. Furthermore, the following statements hold.

1. *The isometry group of any surface $M_{\theta,\alpha,\beta} \in \mathcal{K}$ is isomorphic to $(\mathbb{Z}/2\mathbb{Z})^2$, $(\mathbb{Z}/2\mathbb{Z})^3$, or $(\mathbb{Z}/2\mathbb{Z})^4$, depending on the values of α and β, and it contains an orientation-reversing involution without fixed points producing a quotient Klein bottle with two parallel ends.*
2. *$\mathcal{K}$ is* self-conjugate *in the sense that the conjugate surface of any example in $\mathcal{K}$ also belongs to $\mathcal{K}$.* (Two minimal surfaces $M_1, M_2 \subset \mathbb{R}^3$ are *conjugate* if the coordinate functions of M_2 are harmonic conjugate to the coordinate functions of M_1.)
3. *The possible limits of surfaces in $\mathcal{K}$ are the catenoid, the helicoid, any singly or doubly periodic Scherk minimal surface, any Riemann minimal example, or another surface in $\mathcal{K}$.*

We refer to the examples $M_{\theta,\alpha,\beta}$ in $\mathcal{K}$ as *standard examples.* It is clear that we can consider quotients of the standard examples by less refined period lattices to have $4k$ ends for any natural k, keeping genus 1. Pérez, Rodríguez, and Traizet [9] have proved that these are the only possible examples in this setting.

THEOREM 2 [9]. *If $M \subset \mathbb{R}^3$ is a doubly periodic minimal surface with parallel ends and genus* 1 *in the quotient, then M must be a standard example in $\mathcal{K}$ up to translations, rotations, and homotheties.*

Meeks and Rosenberg [7] developed a general theory for doubly periodic minimal surfaces having finite topology in the quotient. They used an approach of minimax type to prove the existence of new minimal examples with parallel ends and genus 1 in the quotient, besides those given by Karcher. After studying in detail the surfaces in $\mathcal{K}$, the uniqueness Theorem 2 assures that Meeks and Rosenberg's examples are nothing but $M_{\theta,0,\beta}$ for $\beta < \theta$. Thus at least two of the most symmetric 1-parameter families in $\mathcal{K}$ were known by Karcher [3; 4] and by Meeks and Rosenberg [7] (although our approach here is different from theirs). For this reason, the surfaces in $\mathcal{K}$ also appear sometimes in the literature as *KMR examples.*

We will construct all standard examples as branched coverings of the sphere $\mathbb{S}^2$ by their Gauss maps. The *spherical configuration* of a standard example, defined as the position in $\mathbb{S}^2$ of the branch values of its Gauss map, allows us to read all the information concerning the minimal surface; see Section 2. Besides giving a unified method to produce all standard examples and studying their geometry, our motivation for writing this paper was to study the topology of $\mathcal{K}$.

THEOREM 3. *The space $\mathcal{K}$ of properly embedded minimal surfaces with genus* 1 *and parallel ends in $\mathbb{T} \times \mathbb{R}$, $\mathbb{T}$ a 2-dimensional flat torus, is diffeomorphic to $\mathbb{R} \times (\mathbb{R}^2 - \{(\pm 1, 0)\})$.*

The proof of Theorem 3 is inspired by the arguments of Pérez, Rodríguez, and Traizet [9] to prove Theorem 2 (they follow the ideas of Meeks, Pérez, and Ros [6]). We model the family $\mathcal{K}$ of standard examples as an analytic subset in a complex manifold $\mathcal{W}$ of finite dimension (roughly, $\mathcal{W}$ consists of all admissible Weierstrass data for our problem). In the boundary of $\mathcal{K}$ in $\mathcal{W}$, we can find the 1-parameter family $\mathcal{S}$ of singly periodic Scherk minimal surfaces [3; 10]. We consider the classifying map $C\colon \tilde{\mathcal{K}} \to \Lambda = \mathbb{R}^+ \times \mathbb{S}^1 \times \mathbb{R}$, defined on $\tilde{\mathcal{K}} = \mathcal{K} \cup \mathcal{S}$, which associates to each surface in $\tilde{\mathcal{K}}$ two geometric invariants: its period at the ends and its flux along a nontrivial homology class with vanishing period vector. Theorem 3 is a simple consequence of the following statements.

1. $C\colon \tilde{\mathcal{K}} \to \Lambda$ is a proper map.
2. $C\colon \tilde{\mathcal{K}} \to \Lambda$ is a local diffeomorphism.
3. There exists $x \in \Lambda$ such that $C^{-1}(x)$ consists of only one surface in $\tilde{\mathcal{K}}$.
4. $C(\mathcal{S})$ is a proper, divergent curve in Λ.

The paper is organized as follows. In Section 2 we study the family $\mathcal{K}$ of standard examples. Section 3 is devoted to introducing the space $\mathcal{W}$ of admissible Weierstrass data and the classifying map C that we use as a tool to demonstrate Theorem 3; we also prove that C is a proper map. The goal of Section 4 is to prove the second statement above (i.e., that C is a local diffeomorphism). Finally, Theorem 3 is proved in Section 5.

I sincerely want to thank Joaquín Pérez for his invaluable help along these years and for leading me through this work.

2. Standard Examples (Proof of Theorem 1)

We dedicate this section to introducing the 3-parameter family $\mathcal{K}$ of standard examples appearing in Theorem 1, to which the uniqueness Theorem 2 applies. First, let us point out some general facts. Let $\tilde{M} \subset \mathbb{R}^3$ be a doubly periodic minimal surface with period lattice $\mathcal{P}$. Such $\tilde{M}$ induces a properly embedded minimal surface $M = \tilde{M}/\mathcal{P}$ in the complete flat 3-manifold $\mathbb{R}^3/\mathcal{P} = \mathbb{T} \times \mathbb{R}$, where $\mathbb{T}$ is a 2-dimensional flat torus. Conversely, if $M \subset \mathbb{T} \times \mathbb{R}$ is a properly embedded nonflat minimal surface, then its lift $\tilde{M} \subset \mathbb{R}^3$ is a connected doubly periodic minimal surface by the strong half-space theorem of Hoffman and Meeks [2]. Assume that the topology of M is a finitely punctured torus and that its ends are parallel. Then, by Meeks and Rosenberg [7], M must have finite total curvature and $4k$ Scherk-type ends for some natural k. Hence M is conformally equivalent to a torus $\mathbb{M}$ minus $4k$ punctures. If we consider $\mathcal{P}$ to be the more refined period lattice of $\tilde{M}$, then Theorem 2 implies that $k = 1$.

Since M has finite total curvature, its Gauss map g extends meromorphically to $\mathbb{M}$. After a rotation so that the ends of M are horizontal, g takes values $0, \infty$ at the punctures, and the third coordinate function h (which is not well-defined on M) defines a univalent holomorphic 1-form dh on $\mathbb{M}$, which we will call the *height differential*. Meeks and Rosenberg [7] proved that one of the two meromorphic

differentials $g\,dh$, $\frac{dh}{g}$ has a simple pole at each puncture. Since dh has no zeros on $\mathbb{M}$ (it has no poles), we conclude that g is unbranched at the ends and has degree 2. The Riemann–Hurwitz formula implies that the total branching number of g is 4.

Any standard example will be given in terms of the branch values of its Gauss map, which will consist of two pairs of antipodal points D, D', D'', D''' in the sphere $\mathbb{S}^2$. We label those points so that $D'' = -D$ and $D''' = -D'$. Because the Gauss map is unbranched at the ends (which are horizontal), we require that these branch values be different from the North and South Poles. We denote by $e \subset \mathbb{S}^2$ the equator that contains D, D', D'', D''' and by $P \in e$ the point that bisects the angle 2θ between D and D', $\theta \in \left(0, \frac{\pi}{2}\right)$. By a *spherical configuration* we will mean any set $\{D, D', D'', D'''\}$ as just described.

2.1. Toroidal Half-Plane Layers $M_{\theta,0,0}$

With the foregoing notation, given $\theta \in \left(0, \frac{\pi}{2}\right)$ we set the equator e to be the inverse image of the imaginary axis $i\bar{\mathbb{R}} \subset \bar{\mathbb{C}}$ through the stereographic projection from the North Pole, and we set $P = (0, 0, 1)$; see Figure 1 left. After stereographic projection we have $D = -\lambda i$, with $\lambda = \lambda(\theta) = \cot\frac{\theta}{2}$, and the remaining branch values of the Gauss map of the example $M_{\theta,0,0}$ we are constructing are the four roots of the polynomial $(z^2 + \lambda^2)(z^2 + \lambda^{-2})$. Thus the underlying conformal compactification of the potential surface $M_{\theta,0,0}$ is the rectangular torus

$$\Sigma_\theta = \{(z, w) \in \bar{\mathbb{C}}^2 \mid w^2 = (z^2 + \lambda^2)(z^2 + \lambda^{-2})\}.$$

The degree-2 extended Gauss map of $M_{\theta,0,0}$ is $g(z, w) = z$, the punctures correspond to $(0, \pm 1), (\infty, \pm\infty) \in \Sigma_\theta$, and the height differential must be $dh = \mu\frac{dz}{w}$ for certain $\mu = \mu(\theta) \in \mathbb{C}^*$.

We consider $\mu \in \mathbb{R}^*$. Then the set $\{(z, w) \mid |z| = 1\}$ corresponds on $M_{\theta,0,0}$ to two closed horizontal geodesics that are the fixed point set of reflection symmetries S_3 in two horizontal planes (the reflections in both planes induce the same isometry S_3 of the quotient surface); the set $\{(z, w) \mid z \in \mathbb{R}\}$ corresponds on $M_{\theta,0,0}$ to

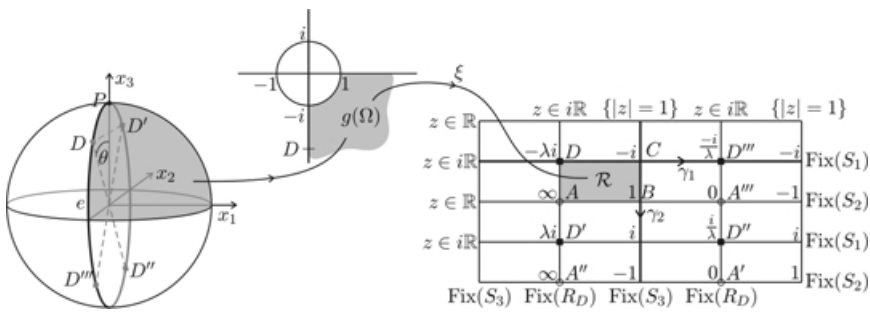

Figure 1 *Left:* Spherical configuration of $M_{\theta,0,0}$ *Center:* The biholomorphism ξ between the shaded regions *Right:* The conformal torus Σ_θ, where Fix$(\cdot)$ denotes fixed point set

four geodesics traveling from a zero to a pole of the Gauss map g that are the fixed point set of a reflection symmetry S_2 across two planes orthogonal to the x_2-axis; and the set $\{(it, w) \mid t \in \mathbb{R},\ \lambda^{-1} \leq |t| \leq \lambda\}$ corresponds to two geodesics that are the fixed point set of a reflection symmetry S_1 in a vertical plane orthogonal to the x_1-axis. These last two geodesics cut orthogonally four straight lines, parallel to the x_1-axis and contained in $M_{\theta,0,0}$, that correspond to the set $\{(it, w) \mid |t| \leq \lambda^{-1}$ or $|t| \geq \lambda\}$. We will denote by R_D the π-rotation around any such straight line (see Figure 4 left).

We now construct a different model of Σ_θ: as a quotient of the ξ-plane $\mathbb{C}$ over a rectangular lattice. Let $\Omega \subset \Sigma_\theta$ be one of the two components of $g^{-1}\big(\{|z| > 1, -\frac{\pi}{2} < \arg(z) < 0\}\big)$. Here Ω is topologically a disk, and its boundary contains the branch point corresponding to the branch value D of g and one of the ends corresponding to a pole of g. Let $\mathcal{R}$ be an open rectangle in the ξ-plane of consecutive vertices $A, B, C, D \in \mathbb{C}$, with the segment $\overline{AB}$ horizontal, such that there exists a biholomorphism $\xi : \{|z| > 1, -\frac{\pi}{2} < \arg(z) < 0\} \to \mathcal{R}$ with boundary values $\xi(\infty) = A$, $\xi(1) = B$, $\xi(-i) = C$, and $\xi(-\lambda i) = D$. Then the composition of g with ξ defines a biholomorphism between Ω and $\mathcal{R}$. After symmetric extension of this biholomorphism across the boundary curves, we will get a biholomorphism from Σ_θ to the quotient of the ξ-plane modulo the translations given by four times the sides of the rectangle $\mathcal{R}$. We abuse notation by using D, D', D'', D''' to label also the points of the ξ-plane that correspond to the branch values of g. The deck transformation $(z, w) \overset{\mathcal{D}}{\mapsto} (z, -w)$ of Σ_θ corresponds in the ξ-plane to the π-rotation about the branch points of g. It will be also useful to see Σ_θ as a branched $2:1$ covering of $\bar{\mathbb{C}}$ through the map $(z, w) \mapsto z$—that is, two copies $\bar{\mathbb{C}}_1, \bar{\mathbb{C}}_2$ of $\bar{\mathbb{C}}$ glued along common cuts from D to D' and from D'' to D''', both contained in the imaginary axis.

In the ξ-plane model of Σ_θ: S_3 corresponds to the reflection across the line passing through B, C (or across its parallel line after translation by half a horizontal period—see Figure 1 right); S_2 is the reflection across the line passing through A, B (or across its parallel line after translation by half a vertical period); S_1 is the reflection across the line passing through D, D''' (or through D', D''); and R_D is the reflection across the line passing through D, D' (or through D'', D'''). It is easy to see that $\mathrm{Iso}(M_{\theta,0,0})$ coincides with the group of conformal transformations of the underlying conformal torus Σ_θ, which is isomorphic to $(\mathbb{Z}/2\mathbb{Z})^4$ with generators S_1, S_2, S_3, R_D.

Remark 1. All surfaces $M_{\theta,\alpha,\beta} \in \mathcal{K}$ to be defined will have the same conformal compactification Σ_θ as $M_{\theta,0,0}$. So from now on the sixteen elements in $\mathrm{Iso}(M_{\theta,0,0})$ generated by S_1, S_2, S_3, R_D will be seen as conformal transformations of Σ_θ. Those that leave invariant the distribution of zeros and poles of the Gauss map of $M_{\theta,\alpha,\beta}$ will be precisely the isometries of this last surface.

Concerning the period problem for $M_{\theta,0,0}$, let γ_1, γ_2 be the simple closed curves in Σ_θ obtained as quotients of the horizontal and vertical lines in the ξ-plane passing through D, D''' and through C, B respectively (see Figure 1 right). Clearly $\{\gamma_1, \gamma_2\}$

is a basis of $H_1(\Sigma_\theta, \mathbb{Z})$. We normalize so that $\int_{\gamma_2} dh = 2\pi i$, which determines dh or (equivalently) the value of μ:

$$\mu = \mu(\theta) = \frac{\pi \csc\theta}{\mathcal{K}(\sin^2\theta)}, \tag{1}$$

where

$$\mathcal{K}(m) = \int_0^{\pi/2} \frac{1}{\sqrt{1 - m\sin^2 u}}\, du, \quad 0 < m < 1,$$

is the complete elliptic integral of the first kind. With this choice of μ, the period and flux vectors of $M_{\theta,0,0}$ along a small loop γ_A around the end $A = (\infty, +\infty) \in \Sigma_\theta$ of $M_{\theta,0,0}$ are respectively

$$P_{\gamma_A} = (0, \pi\mu, 0) \quad \text{and} \quad F_{\gamma_A} = (\pi\mu, 0, 0). \tag{2}$$

The remaining ends of $M_{\theta,0,0}$ are

$$A' = (S_1 \circ S_2 \circ S_3)(A), \quad A'' = \mathcal{D}(A) = (S_1 \circ R_D)(A), \quad A''' = \mathcal{D}(A')$$

(see Figure 1 right). From the behavior of the Weierstrass form $\Phi = \left(\frac{1}{2}\left(\frac{1}{g} - g\right), \frac{i}{2}\left(\frac{1}{g} + g\right), 1\right)dh$ under pullback by S_1, S_2, S_3, R_D, one obtains that

$$\operatorname{Res}_A \Phi = -\overline{\operatorname{Res}_{A'} \Phi} = -\operatorname{Res}_{A''} \Phi = \overline{\operatorname{Res}_{A'''} \Phi}, \tag{3}$$

where Res_X denotes the residue at the point $X \in \Sigma_\theta$. Note that (2) and (3) determine completely the periods and fluxes at A', A'', A''':

$$P_{\gamma_A} = P_{\gamma_{A'}} = -P_{\gamma_{A''}} = -P_{\gamma_{A'''}}, \qquad F_{\gamma_A} = -F_{\gamma_{A'}} = -F_{\gamma_{A''}} = F_{\gamma_{A'''}}. \tag{4}$$

Similar arguments imply that the periods and fluxes along the homology basis are

$$\begin{aligned} P_{\gamma_1} &= (0, 0, f_1), & F_{\gamma_1} &= -F_{\gamma_A} = (-\pi\mu, 0, 0), \\ P_{\gamma_2} &= (0, 0, 0), & F_{\gamma_2} &= (0, 0, 2\pi), \end{aligned} \tag{5}$$

where

$$f_1 = f_1(\theta) = -4\mu \int_1^\lambda \frac{dt}{\sqrt{(t^2 - \lambda^{-2})(\lambda^2 - t^2)}} < 0. \tag{6}$$

From equations (2), (4), and (5) we conclude that $M_{\theta,0,0}$ is a complete immersed minimal surface invariant by the rank-2 lattice generated by $P_{\gamma_A}, P_{\gamma_1}$. Moreover, $M_{\theta,0,0}$ has genus 1 and four horizontal Scherk-type ends in the quotient, and it can be decomposed into 16 congruent disjoint pieces. Karcher [3] proved that each of these pieces is the conjugate surface of certain Jenkins–Serrin graph defined on a convex domain. In particular, $M_{\theta,0,0}$ is embedded.

Next we study the limit surfaces of the examples in the family $\left\{M_{\theta,0,0} \mid \theta \in \left(0, \frac{\pi}{2}\right)\right\}$. When θ goes to 0, the function $\lambda(\theta)$ diverges to $+\infty$. After changing variables $(z, w) \in \Sigma_\theta$ for (z, w_1) with $w_1\lambda(\theta) = w$, it is easy to see that Σ_θ degenerates as $\theta \to 0^+$ into two spheres $\{(z, w_1) \mid w_1^2 = z^2\}$. The limiting Gauss map of $M_{\theta,0,0}$ as $\theta \to 0^+$ is $g(z, w_1) = z$, and the height differential dh of $M_{\theta,0,0}$ converges smoothly to $\frac{dz}{w_1} = \pm\frac{dz}{z}$. Hence, when $\theta \to 0^+$, the example $M_{\theta,0,0}$ converges smoothly to two vertical catenoids with flux $(0, 0, 2\pi)$; see Figure 2 left.

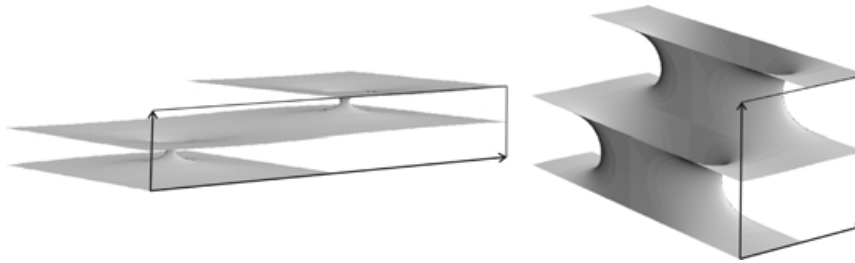

Figure 2 $M_{\theta,0,0}$ for $\theta = \frac{\pi}{50}$ (left) and for $\theta = \frac{24\pi}{50}$ (right)

If $\theta \to \left(\frac{\pi}{2}\right)^-$, then $\lambda(\theta) \to 1$ and Σ_θ degenerates into two spheres $\{(z,w) \mid w^2 = (z^2+1)^2\}$. In this case, the limiting Gauss map is $g(z,w) = z$ and the height differential collapses to zero because the limit of $\mu(\theta)$ when $\theta \to \left(\frac{\pi}{2}\right)^-$ vanishes. After scaling, it holds that $\frac{1}{\mu(\theta)} dh \to \pm\frac{dz}{z^2+1}$ as $\theta \to \left(\frac{\pi}{2}\right)^-$. Therefore, after blowing up, $M_{\theta,0,0}$ converges smoothly as $\theta \to \left(\frac{\pi}{2}\right)^-$ to two doubly periodic Scherk minimal surfaces with two horizontal and two vertical ends (see Figure 2 right).

2.2. The Examples $M_{\theta,\alpha,\beta}$

Given $\theta \in \left(0, \frac{\pi}{2}\right)$, $\alpha \in \left[0, \frac{\pi}{2}\right]$, and $\beta \in \left[0, \frac{\pi}{2}\right]$ with $(\alpha,\beta) \neq (0,\theta)$, we consider the equator e to be the rotated image of the imaginary axis in the sphere by angle α around the x_2-axis. If we denote by Q the rotated point by angle α around the x_2-axis of the North Pole, then our new point P will be the rotation of Q by angle β along e; see Figure 3 left. Note that if $(\alpha,\beta) = (0,\theta)$ then D' coincides with the North Pole, which is not allowed in this setting. Also note that the spherical configuration $\{D, D', D'', D'''\}$ associated to θ, α, β is nothing but the rotated image of that of $M_{\theta,0,0}$ by the Möbius transformation ϕ corresponding to the composition of the rotation of angle β around the x_1-axis with the rotation of angle α around the x_2-axis. Consequently, we define the Gauss map $g = g_{\theta,\alpha,\beta}$ of the standard example $M_{\theta,\alpha,\beta}$ we want to construct as $g = \phi \circ g_{\theta,0,0}$; that is,

$$g(z,w) = \frac{\sigma z + \delta}{i(\bar{\sigma} - \bar{\delta} z)}$$

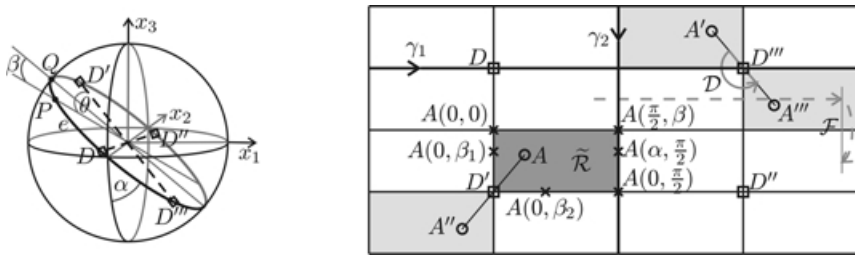

Figure 3 *Left:* Spherical configuration of $M_{\theta,\alpha,\beta}$ *Right:* The ξ-plane model of Σ_θ, where the dotted line represents the isometry $\mathcal{F}$ and where $\alpha \in \left(0, \frac{\pi}{2}\right)$, $\beta \in \left[0, \frac{\pi}{2}\right]$, and $0 < \beta_1 < \theta < \beta_2 < \frac{\pi}{2}$

for $(z,w)\in\Sigma_\theta$, where $\sigma=\cos\left(\frac{\alpha+\beta}{2}\right)+i\cos\left(\frac{\alpha-\beta}{2}\right)$ and $\delta=\sin\left(\frac{\alpha-\beta}{2}\right)+i\sin\left(\frac{\alpha+\beta}{2}\right)$. Since g depends analytically on α,β, the same holds for its zeros and poles. We will denote by $\{A,A',A'',A'''\}=g^{-1}(\{0,\infty\})$ the ends of $M_{\theta,\alpha,\beta}$, understanding that each zero or pole of g is defined by analytical continuation of the corresponding zero or pole of $g_{\theta,0,0}$. Choosing the same homology class $[\gamma_2]\in H_1(\Sigma_\theta,\mathbb{Z})$ as in Section 2.1, we obtain that the height differential of $M_{\theta,\alpha,\beta}$ is $dh=\mu\frac{dz}{w}$, with $\mu=\mu(\theta)$ as in (1). Thus, the Weierstrass data of $M_{\theta,\alpha,\beta}$ coincides with those of $M_{\theta,0,0}$ when $\alpha=\beta=0$.

The group $\mathrm{Iso}(M_{\theta,\alpha,\beta})$ of isometries of the induced metric by (g,dh) always contains the deck transformation $\mathcal{D}=S_1\circ R_D$ (we follow the notation in Section 2.1; see Remark 1). Furthermore, the antipodal map in $\mathbb{S}^2$ leaves invariant the spherical configuration of $M_{\theta,\alpha,\beta}$, so $\mathrm{Iso}(M_{\theta,\alpha,\beta})$ also contains two antiholomorphic involutions without fixed points, $\mathcal{E}$ and $\mathcal{F}=\mathcal{E}\circ\mathcal{D}$. It is straightforward to check that we can label $\mathcal{E}=S_1\circ S_2\circ S_3$ and hence $\mathcal{F}=R_D\circ S_2\circ S_3$. This information is enough to solve the period problem for $M_{\theta,\alpha,\beta}$.

The period and flux vectors of $M_{\theta,\alpha,\beta}$ at the end A are given by

$$P_{\gamma_A}=\pi\mu\sin\theta(iE(\theta,\alpha,\beta),0)\quad\text{and}\quad F_{\gamma_A}=\pi\mu\sin\theta(E(\theta,\alpha,\beta),0),\qquad(7)$$

where we have used the identification of $\mathbb{R}^3$ with $\mathbb{C}\times\mathbb{R}$ by $(a,b,c)\equiv(a+ib,c)$, and

$$E(\theta,\alpha,\beta)=\frac{1}{\sqrt{\sin^2\theta\cos^2\alpha+(\sin\alpha\cos\beta-i\sin\beta)^2}}.$$

The periods and fluxes at the remaining ends $A'=\mathcal{E}(A)$, $A''=\mathcal{D}(A)$, and $A'''=\mathcal{F}(A)$ can be obtained from the equations in (4), which are still valid.

We choose the homology classes $[\gamma_1],[\gamma_2]\in H_1(\Sigma_\theta,\mathbb{Z})$ as in Section 2.1 (note that we can even take the same curve representatives γ_1,γ_2 as in the case $\alpha=\beta=0$ except when $\alpha=\frac{\pi}{2}$ or $\beta=\frac{\pi}{2}$). In particular, the third coordinate $(P_{\gamma_1})_3$ of the period of $M_{\theta,\alpha,0}$ along γ_1 equals f_1, given by (6), so P_{γ_A} and P_{γ_1} are linearly independent. Also,

$$\mathcal{E}^*\Phi=-\bar{\Phi},\quad \mathcal{E}_*\gamma_1=-\gamma_1-\gamma_A-\gamma_{A'''},\quad \mathcal{E}_*\gamma_2=\gamma_2,\qquad(8)$$

where Φ denotes the Weierstrass form for $M_{\theta,\alpha,\beta}$. Equalities in (8) and (3) imply that $\overline{\int_{\gamma_1}\Phi}=\int_{\gamma_1}\Phi+\int_{\gamma_A}\Phi-\overline{\int_{\gamma_A}\Phi}$ and $\int_{\gamma_2}\Phi=-\overline{\int_{\gamma_2}\Phi}$, from which we deduce

$$F_{\gamma_1}=-F_{\gamma_A}\quad\text{and}\quad P_{\gamma_2}=(0,0,0).\qquad(9)$$

All of these facts imply that $M_{\theta,\alpha,\beta}$ is a complete immersed minimal torus invariant by the rank-2 lattice generated by $P_{\gamma_A}, P_{\gamma_1}$, which has four horizontal Scherk-type ends in the quotient. Since $M_{\theta,0,0}$ is embedded and since the heights of the ends of $M_{\theta,\alpha,\beta}$ depend continuously on (α,β), which are in the connected set $\left[0,\frac{\pi}{2}\right]^2-\{(0,\theta)\}$, we deduce that $M_{\theta,\alpha,\beta}$ is embedded outside a fixed compact set. This fact together with a standard application of the maximum principle ensures that $M_{\theta,\alpha,\beta}$ is embedded for all values of θ,α,β.

We next discuss what constitutes the list of isometries of $M_{\theta,\alpha,\beta}$ for different values of θ,α,β. As mentioned previously, $\mathrm{Iso}(M_{\theta,\alpha,\beta})$ always contains the subgroup $\{\text{identity},\mathcal{D},\mathcal{E},\mathcal{F}\}$, which is isomorphic to $(\mathbb{Z}/2\mathbb{Z})^2$ with generators $\mathcal{D},\mathcal{F}$.

The deck transformation $\mathcal{D}$ represents in $\mathbb{R}^3$ a central symmetry about any of the four branch points of g, and $\mathcal{F}$ consists of a translation by $\frac{1}{2}(P_{\gamma_A} + P_{\gamma_1})$. In particular, the ends of $M_{\theta,\alpha,\beta}$ are equally spaced. If $0 < \beta < \frac{\pi}{2}$ and $0 < \alpha < \frac{\pi}{2}$, then the puncture $A = A(\alpha, \beta)$ lies on the open rectangle $\tilde{\mathcal{R}} = S_2(\mathcal{R})$; see Figure 3 right. By Remark 1, $\mathrm{Iso}(M_{\theta,\alpha,\beta})$ does not contain either S_1, S_2, S_3, or R_D for these values of θ, α, β and so $\mathrm{Iso}(M_{\theta,\alpha,\beta}) = \{\text{identity}, \mathcal{D}, \mathcal{E}, \mathcal{F}\}$. Thus it remains to study the special cases $\alpha \in \left\{0, \frac{\pi}{2}\right\}$ and $\beta \in \left\{0, \frac{\pi}{2}\right\}$. We proceed in six steps as follows.

1. The case $\alpha = \beta = 0$ was studied in Section 2.1.

2. Suppose that $\alpha = 0$ and that $0 < \beta < \frac{\pi}{2}$ for $\beta \neq \theta$. In the ξ-plane model of Σ_θ, the puncture A moves vertically from its original position at the upper left corner of $\tilde{\mathcal{R}}$ when $\beta = 0$ downward until collapsing for $\beta = \theta$ with the branch point D'. Next it goes on moving horizontally to the right until reaching the lower right corner of $\tilde{\mathcal{R}}$ for $\beta = \frac{\pi}{2}$ (see Figure 3 right). The group of isometries $\mathrm{Iso}(M_{\theta,0,\beta})$ is isomorphic to $(\mathbb{Z}/2\mathbb{Z})^3$ with generators S_1, R_D, and $R_1 = S_2 \circ S_3$. Here S_1 represents in $\mathbb{R}^3$ (as in Section 2.1) a reflection symmetry across a plane orthogonal to the x_1-axis, and R_1 corresponds to a π-rotation in $\mathbb{R}^3$ around a line parallel to the x_1-axis that cuts the surface orthogonally. When $0 < \beta < \theta$ $\left(\text{resp. } \theta < \beta < \frac{\pi}{2}\right)$, $M_{\theta,0,\beta}$ contains four (resp. two) straight lines parallel to the x_1-axis; see Figure 4 right (resp. Figure 5 left). In both cases, R_D is the π-rotation around any such line.

3. In the case where $\alpha = 0$ and $\beta = \frac{\pi}{2}$, the puncture A coincides with the lower right corner of $\tilde{\mathcal{R}}$, and $\mathrm{Iso}(M_{\theta,0,\pi/2}) = \mathrm{Iso}(M_{\theta,0,0})$. The isometry S_1 represents in $\mathbb{R}^3$ a reflection symmetry across a plane orthogonal to the x_1-axis. In this case, S_3

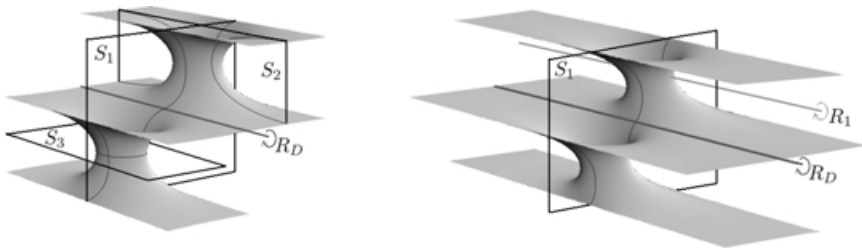

Figure 4 *Left:* $M_{\theta,0,0}$ for $\theta = \frac{\pi}{4}$ *Right:* $M_{\theta,0,\beta}$ for $\theta = \frac{\pi}{4}$ and $\beta = \frac{\pi}{8}$

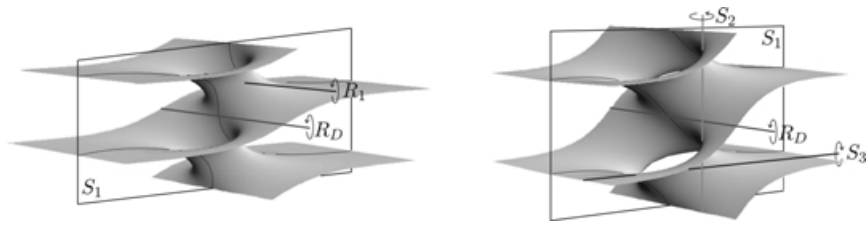

Figure 5 *Left:* $M_{\theta,0,\beta}$ for $\theta = \frac{\pi}{4}$ and $\beta = \frac{3\pi}{8}$ *Right:* $M_{\theta,0,\beta}$ for $\theta = \frac{\pi}{4}$ and $\beta = \frac{\pi}{2}$

(resp. S_2) represents in $\mathbb{R}^3$ a π-rotation around one of the four (resp. two) straight lines parallel to the x_2-axis (resp. x_3-axis) contained on $M_{\theta,0,\pi/2}$; see Figure 5 right.

4. If $0 < \alpha < \frac{\pi}{2}$ and $\beta = \frac{\pi}{2}$ then S_3 is an isometry of (g, dh), since A moves from the lower right corner of $\tilde{\mathcal{R}}$ to its upper right corner as α varies from 0 to $\frac{\pi}{2}$. And $\mathrm{Iso}(M_{\theta,\alpha,\pi/2})$ is isomorphic to $(\mathbb{Z}/2\mathbb{Z})^3$ with generators S_3, $\mathcal{D}$, and $R_3 = S_1 \circ S_2$. Now S_3 represents in $\mathbb{R}^3$ a π-rotation around any of the four straight lines parallel to the x_2-axis contained on $M_{\theta,\alpha,\pi/2}$, and R_3 is the composition of a reflection symmetry across a plane orthogonal to the x_2-axis with a translation by half a horizontal period; see Figure 6.

Figure 6 The standard example $M_{\theta,\alpha,\beta}$ for $\theta = \alpha = \frac{\pi}{4}$ and $\beta = \frac{\pi}{2}$

5. Suppose now that $0 < \alpha < \frac{\pi}{2}$ and $\beta = 0$. Then the puncture A moves horizontally to the right running along the upper boundary side of $\tilde{\mathcal{R}}$. Thus $\mathrm{Iso}(M_{\theta,\alpha,0})$ is isomorphic to $(\mathbb{Z}/2\mathbb{Z})^3$, with generators S_2, $\mathcal{D}$, and $R_2 = S_1 \circ S_3$. As in the case of $M_{\theta,0,0}$, here S_2 represents in space a reflection symmetry across two planes orthogonal to the x_2-axis, and R_2 is a π-rotation around a line parallel to the x_2-axis that cuts $M_{\theta,\alpha,0}$ orthogonally; see Figure 7 left.

6. If $\alpha = \frac{\pi}{2}$, then $M_{\theta,\pi/2,\beta}$ is nothing but the rotated image of $M_{\theta,\pi/2,0}$ by angle β around the x_3-axis. Hence we reduce the study to $\beta = 0$. Now A lies on the upper right corner of $\tilde{\mathcal{R}}$, so all S_1, S_2, S_3, R_D leave invariant the distribution of zeros and poles of the Gauss map of $M_{\theta,\pi/2,\beta}$, and $\mathrm{Iso}(M_{\theta,\pi/2,\beta}) = \mathrm{Iso}(M_{\theta,0,0})$. In

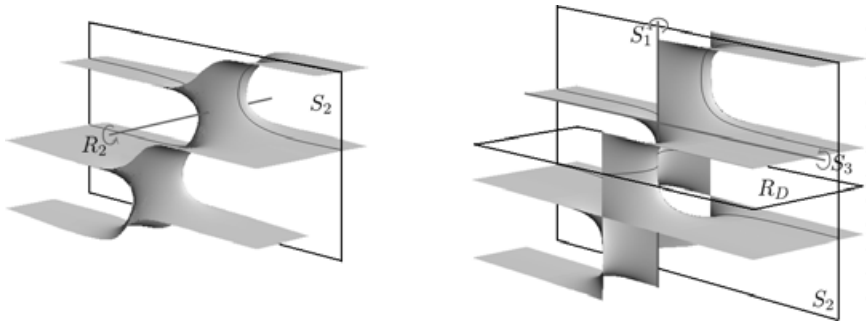

Figure 7 *Left:* $M_{\theta,\alpha,0}$ for $\theta = \alpha = \frac{\pi}{4}$ *Right:* $M_{\theta,\alpha,0}$ for $\theta = \frac{\pi}{4}$ and $\alpha = \frac{\pi}{2}$

this case S_2 represents a reflection symmetry across two planes orthogonal to the x_2-axis, S_3 (resp. S_1) represents in $\mathbb{R}^3$ a π-rotation around one of the four (resp. two) straight lines parallel to the x_1-axis (resp. x_3-axis) contained on $M_{\theta,\pi/2,0}$, and R_D corresponds to a reflection symmetry across two horizontal planes; see Figure 7 right.

Next let us show a uniqueness result used in the proof of Theorem 3 (Section 5).

LEMMA 1. *With notation as before,* $F_{\gamma_2} = (0, 0, 2\pi)$ *if and only if* $\alpha = \beta = 0$.

Proof. From (5) we know that $F_{\gamma_2} = (0, 0, 2\pi)$ when $\alpha = \beta = 0$. Now suppose that $F_{\gamma_2} = (0, 0, 2\pi)$ and let us conclude that both α and β vanish.

If $\beta = \frac{\pi}{2}$, then R_3 is an isometry of $M_{\theta,\alpha,\beta}$ and we have $\gamma_2 - (R_3)_*\gamma_2 = \gamma_{A'} - \gamma_A$ and $R_3^*\Phi = (\phi_1, -\phi_2, \phi_3)$. Moreover, we obtain from (4) and (7) that $P_{\gamma_A} = P_{\gamma_{A'}}$ and $-F_{\gamma_A} = F_{\gamma_{A'}} = (0, \pi a, 0)$, with $a = (\mu \sin\theta)\big/\sqrt{1 - \sin^2\theta\cos^2\alpha} > 0$. Thus

$$\int_{\gamma_2} \Phi = \int_{\gamma_2} (\phi_1, -\phi_2, \phi_3) + 2i(0, \pi a, 0),$$

and the second component of F_{γ_2} equals $\pi a \neq 0$, which is not possible. Therefore, $\beta \neq \frac{\pi}{2}$. Since $M_{\theta,\pi/2,\beta}$ differs from $M_{\theta,\pi/2,\pi/2}$ in a rotation about the x_3-axis, we also have $\alpha \neq \frac{\pi}{2}$. That is, $\alpha, \beta \in \left[0, \frac{\pi}{2}\right)$, and we can choose for every α, β the same curve representative γ_2 as in the case $\alpha = \beta = 0$ (i.e., $\gamma_2 = \{z \in \bar{\mathbb{C}}_1 \mid |z| = 1\}$).

Since $P_{\gamma_2} = (0, 0, 0)$, it follows that $F_{\gamma_2} = \left(i\int_{\gamma_2} g\, dh, 2\pi\right) \in \mathbb{C} \times \mathbb{R}$ and

$$0 = \int_{\gamma_2} g\, dh = -2\mu \int_{-\pi}^{\pi} \frac{\cos\beta \sin t + i(\sin\alpha \sin\beta \sin t - \cos\alpha \cos t)}{|\sigma - \delta e^{-it}|^2 \sqrt{\lambda^2 + \lambda^{-2} + 2\cos(2t)}}\, dt. \quad (10)$$

Therefore, we deduce from $\Re\left(\int_{\gamma_2} g\, dh\right) = 0$ that

$$\int_0^{\pi} \left(\frac{1}{|\sigma - \delta e^{-it}|^2} - \frac{1}{|\sigma - \delta e^{it}|^2}\right) \frac{\sin t}{\sqrt{\lambda^2 + \lambda^{-2} + 2\cos(2t)}}\, dt$$
$$= 4\sin\beta \int_0^{\pi} \frac{\sin^2 t}{|\sigma - \delta e^{-it}|^2 |\sigma - \delta e^{it}|^2 \sqrt{\lambda^2 + \lambda^{-2} + 2\cos(2t)}}\, dt = 0.$$

The only possibility is then $\beta = 0$, and equation (10) reduces to

$$2\mu i \cos\alpha \int_{-\pi}^{\pi} \frac{\cos t}{|\sigma - \delta e^{-it}|^2 \sqrt{\lambda^2 + \lambda^{-2} + 2\cos(2t)}}\, dt = 0.$$

This is equivalent to

$$\int_0^{\pi} \left(\frac{1}{|\sigma - \delta e^{-it}|^2} + \frac{1}{|\sigma - \delta e^{it}|^2}\right) \frac{\cos t}{\sqrt{\lambda^2 + \lambda^{-2} + 2\cos(2t)}}\, dt$$
$$= 2\sin\alpha \int_0^{\pi/2} \frac{\left(\frac{1}{|\sigma - \delta e^{-it}|^2 |\sigma + \delta e^{it}|^2} + \frac{1}{|\sigma - \delta e^{it}|^2 |\sigma + \delta e^{-it}|^2}\right) \cos t}{\sqrt{\lambda^2 + \lambda^{-2} + 2\cos(2t)}}\, dt = 0,$$

which is satisfied only for $\alpha = 0$. Hence $\alpha = \beta = 0$, as we wanted to prove. □

We finalize this section by listing the possible degenerate limits of the standard examples $M_{\theta,\alpha,\beta}$, all of which can be directly computed by using the Weierstrass data.

- If $(\theta,\beta)\to(\theta_0,\theta_0)$ for some $\theta_0\in\left(0,\frac{\pi}{2}\right)$, then $M_{\theta,0,\beta}$ converges smoothly to a Riemann minimal example.
- If $\theta\to 0^+$ and $(\alpha,\beta)\to(0,0)$, then $M_{\theta,\alpha,\beta}$ converges smoothly to two catenoids with flux $(0,0,2\pi)$; see Figure 2 left.
- If $\theta\to 0^+$ and $(\alpha,\beta)\to(\alpha_0,\beta_0)\neq(0,0)$, then $M_{\theta,\alpha,\beta}$ converges smoothly to two copies of the singly periodic Scherk minimal surfaces with four ends, two of them horizontal, and with angle $\arccos(\cos\alpha_0\cos\beta_0)$; see Figure 8. (Here the *angle* of any singly or doubly periodic Scherk minimal surface is the angle between its nonparallel ends.)

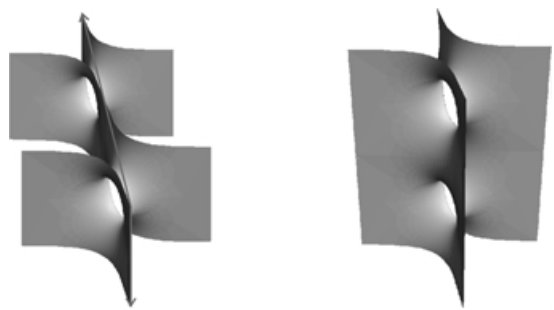

Figure 8 Rotated image of $M_{\theta,0,\beta}$ (left) and two copies of the half of such a rotated $M_{\theta,0,\beta}$ (right) for $\theta=\frac{\pi}{200}$ and $\beta=\frac{9\pi}{20}$

Figure 9 $M_{\theta,0,\beta}$ for $\theta=\frac{19\pi}{40}$ and $\beta=\frac{\pi}{2}$

- If $\theta\to\left(\frac{\pi}{2}\right)^-$ and $(\alpha,\beta)\to\left(0,\frac{\pi}{2}\right)$, then $M_{\theta,\alpha,\beta}$ converges smoothly (after blowing up) to two vertical helicoids spinning oppositely; see Figure 9.
- If $\theta\to\left(\frac{\pi}{2}\right)^-$ and $(\alpha,\beta)\to(\alpha_0,\beta_0)\neq\left(0,\frac{\pi}{2}\right)$, then $M_{\theta,\alpha,\beta}$ converges smoothly (after blowing up) to two copies of the doubly periodic Scherk minimal surfaces with four ends, two of them horizontal, and with angle $\arccos(\cos\alpha_0\sin\beta_0)$; see Figure 2 right.

REMARK 2. We have defined the 3-parametric family $\{M_{\theta,\alpha,\beta}\mid(\theta,\alpha,\beta)\in\mathcal{I}_1\}$ of doubly periodic minimal surfaces with

$$\mathcal{I}_1=\left\{(\theta,\alpha,\beta)\in\left(0,\tfrac{\pi}{2}\right)\times\left[0,\tfrac{\pi}{2}\right]^2\mid(\alpha,\beta)\neq(0,\theta)\right\},$$

and in this range of parameters the end $A = A(\theta, \alpha, \beta)$ runs entirely along the closure of $\tilde{\mathcal{R}}$ except for its lower left corner D'. We can identify $\tilde{\mathcal{R}}$ conformally through the z-map with an octant of $\mathbb{S}^2$. It is easy to extend the range of parameters so that A runs entirely along the sphere minus the branch values of the z-map, which can be achieved by varying (θ, α, β) in

$$\mathcal{I}_2 = \left\{(\theta, \alpha, \beta) \in \left(0, \tfrac{\pi}{2}\right) \times \left[-\tfrac{\pi}{2}, \tfrac{\pi}{2}\right] \times [-\pi, \pi] \mid (\alpha, \beta) \neq (0, \pm\theta), (0, \pm(\pi - \theta))\right\}.$$

We can define $M_{\theta,\alpha,\beta}$ for $(\theta, \alpha, \beta) \in \mathcal{I}_2$ similarly as for $(\theta, \alpha, \beta) \in \mathcal{I}_1$, yet it is straightforward to check that—up to translations, rotations, and homotheties—the following statements hold.

- $M_{\theta,-\pi/2,\beta}$ coincides with $M_{\theta,\pi/2,\beta}$, which does not depend on β.
- $M_{\theta,-\alpha,0}$ is the reflected image of $M_{\theta,\alpha,\beta}$ with respect to a plane that is orthogonal to the x_1-axis.
- $M_{\theta,\alpha,\beta\pm\pi}$ coincides with $M_{\theta,\alpha,\beta}$.
- $M_{\theta,0,-\beta}$ is the reflected image of $M_{\theta,\alpha,\beta}$ with respect to a plane that is orthogonal to the x_2-axis.

Therefore, we define the family of standard examples as $\mathcal{K} = \{M_{\theta,\alpha,\beta} \mid (\theta, \alpha, \beta) \in \mathcal{I}\}$, where

$$\begin{aligned}\mathcal{I} = &\left\{(\theta, \alpha, \beta) \in \left(0, \tfrac{\pi}{2}\right) \times \left(\tfrac{-\pi}{2}, \tfrac{\pi}{2}\right) \times [0, \pi) \mid (\alpha, \beta) \neq (0, \theta), (0, \pi - \theta)\right\} \\ &\cup \left\{\left(\theta, \tfrac{\pi}{2}, 0\right) \mid \theta \in \left(0, \tfrac{\pi}{2}\right)\right\}. \end{aligned} \tag{11}$$

We choose this space of parameters to avoid repeating surfaces twice; see Remark 2.

Remark 3. By construction, the branch values of the Gauss map N of $M_{\theta,\alpha,\beta}$ are contained in a spherical equator of $\mathbb{S}^2$, so a consequence of [8, Thm. 14] assures that the space of bounded Jacobi functions on M coincides with the space of linear functions of N, $\{\langle N, V\rangle \mid V \in \mathbb{R}^3\}$ (in particular, such space is 3-dimensional). In the literature, this condition is usually referred to as the *nondegeneracy* of $M_{\theta,\alpha,\beta}$, which can be interpreted by means of an implicit function theorem argument to obtain that $\mathcal{K}$ is a 3-dimensional real analytic manifold (see Hauswirth and Traizet [1]).

2.3. The Space of Standard Examples Is Self-Conjugate

In the previous section we defined the family $\mathcal{K} = \{M_{\theta,\alpha,\beta} \mid (\theta, \alpha, \beta) \in \mathcal{I}\}$ of standard examples. Given $M_{\theta,\alpha,\beta} \in \mathcal{K}$ with Weierstrass data (g, dh), we let $M^*_{\theta,\alpha,\beta}$ denote the conjugate surface of $M_{\theta,\alpha,\beta}$, with Weierstrass data (g, idh). Taking into account that the flux vector (resp. the period vector) of the conjugate surface along a given curve in the parameter domain equals the period vector (resp. the opposite of the flux vector) of the original surface along the same curve, we deduce from (4), (7), and (9) that $M^*_{\theta,\alpha,\beta}$ is a complete immersed torus invariant by the rank-2 lattice generated by the horizontal vector $P^*_{\gamma_A} = -F_{\gamma_A}$ and $P^*_{\gamma_2} = -F_{\gamma_2}$ (whose third coordinate is -2π) and that it has four horizontal Scherk-type ends in the quotient. Moreover, $M^*_{\theta,\alpha,\beta}$ is embedded thanks to the maximum principle, since

the heights of its ends depend continuously on (α, β) and since $M^*_{\theta,0,0}$ is embedded (it is composed of congruent blocks that are Jenkins–Serrin graphs).

Note that, by (9), the period vector of $M^*_{\theta,\alpha,\beta}$ along $\gamma_2^* = \gamma_1 + \gamma_A$ vanishes and that the third component of the flux of $M^*_{\theta,\alpha,\beta}$ along γ_2^* equals $f_1(\theta)$ as given by (6). The next lemma ensures that, after scaling and rotating the surfaces around the x_3-axis, the families $\mathcal{K}$ and $\mathcal{K}^* = \{M^*_{\theta,\alpha,\beta} \mid (\theta,\alpha,\beta) \in \mathcal{I}\}$ coincide; this will finish the proof of Theorem 1.

LEMMA 2. *Given $(\theta,\alpha,\beta) \in \mathcal{I}_1$, the surface $M_{\pi/2-\theta,\alpha,\beta+\pi/2}$ coincides with $M^*_{\theta,\alpha,\beta}$ up to normalizations.*

Proof. It is easy to see that $\Sigma_{\pi/2-\theta} = \{(\tilde{z},\tilde{w}) \mid \tilde{w}^2 = (\tilde{z}^2-1)^2 + 4\tilde{z}^2\sec^2\theta\}$. Since the Möbius transformation $\varphi(z) = \frac{1-iz}{z-i}$ takes the set of branch points of the z-projection of Σ_θ bijectively to the set of branch points of the $\tilde{z}$-projection of $\Sigma_{\pi/2-\theta}$, it follows that $\Theta(z,w) = (\varphi(z), \tilde{w}(\varphi(z)))$ is a biholomorphism between Σ_θ and $\Sigma_{\pi/2-\theta}$. On the other hand, it is straightforward to check that $g_{\theta,\alpha,\beta} = g_{\pi/2-\theta,\alpha,\beta-\pi/2} \circ \Theta$, where the subindex indicates the parameters of the standard example $M_{\theta,\alpha,\beta}$ for which the corresponding $g_{\theta,\alpha,\beta}$ is the Gauss map. Denoting by dh_θ its height differential (recall that it depends only on θ), a direct computation gives

$$\Theta^* dh_{\pi/2-\theta} = -\frac{\mu\left(\frac{\pi}{2}-\theta\right)}{\mu(\theta)\tan\theta} i dh_\theta = -\frac{K(\sin^2\theta)}{K(\cos^2\theta)} i dh_\theta.$$

Hence $M_{\pi/2-\theta,\alpha,\beta-\pi/2} = M^*_{\theta,\alpha,\beta}$ up to normalizations. Since $M_{\pi/2-\theta,\alpha,\beta-\pi/2} = M_{\pi/2-\theta,\alpha,\beta+\pi/2}$ by Remark 2, the lemma is proved. □

3. The Classifying Map

The surfaces in $\mathcal{K}$ can be naturally seen inside the 4-dimensional complex manifold $\mathcal{W}$ consisting roughly of all admissible Weierstrass data in the setting of Theorem 2.

DEFINITION 1. We denote by $\mathcal{W}$ the space of tuples $(\mathbb{M}, g; p_1, p_2, q_1, q_2, [\gamma])$, where g is a degree-2 meromorphic map defined on a torus $\mathbb{M}$ that is unbranched at its zeros p_1, p_2 and at its poles q_1, q_2 and where $[\gamma]$ is a homology class in $\mathbb{M} - \{p_1, p_2, q_1, q_2\}$ that is not trivial in $H_1(\mathbb{M}, \mathbb{Z})$.

See [9] for a detailed description of $\mathcal{W}$. We will simply use g to denote the elements in $\mathcal{W}$ and call them *marked meromorphic maps*. Each $g = (\mathbb{M}, g; p_1, p_2, q_1, q_2, [\gamma]) \in \mathcal{W}$ determines a unique holomorphic differential $\phi = \phi(g)$ on $\mathbb{M}$ such that

$$\int_\gamma \phi = 2\pi i, \tag{12}$$

since the complex space of holomorphic differentials on $\mathbb{M}$ has dimension 1. Thus each $g \in \mathcal{W}$ can be seen as the Weierstrass data (g, ϕ), defined on $g^{-1}(\mathbb{C}^*)$, of a potential surface in the setting of Theorem 2. Equation (12) means that the period

vector of (g,ϕ) along γ is horizontal and that its flux along γ has third coordinate 2π.

DEFINITION 2. We will say that $g \in \mathcal{W}$ *closes periods* when the following equations hold:

$$\int_\gamma \frac{\phi}{g} = \overline{\int_\gamma g\phi} \quad \text{and} \quad \operatorname{Res}_{p_1} \frac{\phi}{g} = -\operatorname{Res}_{q_1}(g\phi) = a \quad \text{for some } a \in \mathbb{R}^+. \tag{13}$$

Note that the first equation in (13), together with (12), says that $P_\gamma = (0,0,0)$ and $F_\gamma = \left(i\int_\gamma g\phi, 2\pi\right) \in \mathbb{C}\times\mathbb{R}$. The next lemma justifies the preceding definition of closing periods.

LEMMA 3 [9]. *If $g \in \mathcal{W}$ closes periods, then (g,ϕ) is the Weierstrass pair of a properly immersed minimal surface $M \subset \mathbb{T}\times\mathbb{R}$, for a certain flat torus $\mathbb{T}$, with total curvature 8π and four horizontal Scherk-type ends. Furthermore, the fluxes at the ends p_j, q_j are equal to $(-1)^{j+1}(\pi a, 0, 0)$ for the positive real number a appearing in* (13) *for $j = 1, 2$.*

Next we describe how to see each standard example $M_{\theta,\alpha,\beta}$ as an element of $\mathcal{W}$ that closes periods. In a first step we rotate $M_{\theta,\alpha,\beta}$ about the x_3-axis so that the period P_{γ_A} at its end A (we follow the notation in Section 2) is $(0,\pi a,0)$ for certain $a > 0$. Now we associate to $M_{\theta,\alpha,\beta}$ the marked meromorphic map

$$(\Sigma_\theta, g;\, A''' = \mathcal{F}(A),\, A' = \mathcal{E}(A),\, A,\, A'' = \mathcal{D}(A),\, [\gamma_2]),$$

where everything has been already defined in Section 2.2 except the homology class $[\gamma_2]$. Recall that the ends A, A', A'', A''' depend continuously on α, β and that we described explicitly the loop γ_2 for $\alpha = \beta = 0$. For the remaining values of α, β, we take an embedded closed curve $\gamma_2 \subset \Sigma_\theta - \{A, A', A'', A'''\}$ depending continuously on α, β such that $[\gamma_2]$ remains constant in $H_1(\Sigma_\theta, \mathbb{Z})$.

3.1. The Ligature Map

We define the *ligature map* to the holomorphic map $L\colon \mathcal{W} \to \mathbb{C}^4$ given by

$$L(g) = \left(\operatorname{Res}_{p_1}\frac{\phi}{g}, \operatorname{Res}_{q_1}(g\phi), \int_\gamma \frac{\phi}{g}, \int_\gamma g\phi\right),$$

which clearly distinguishes when a marked meromorphic map closes periods:

> A marked meromorphic map $g \in \mathcal{W}$ closes periods if and only if there exist $a \in \mathbb{R}^+$ and $b \in \mathbb{C}$ such that $L(g) = (a, -a, \bar{b}, b)$.

Since the residues of a meromorphic differential on a compact Riemann surface add up to zero, if the second equation in (13) holds then $\operatorname{Res}_{p_2}\frac{\phi}{g} = -\operatorname{Res}_{q_2}(g\phi) = -a$.

Let $\mathcal{S} = \{S_\rho \mid \rho \in (0,\pi)\}$ be the 1-dimensional moduli space of singly periodic Scherk minimal surfaces with two horizontal ends, with the vertical part of the flux at its two nonhorizontal ends equal to 2π and with period vector in the direction of the x_2-axis. For each $\rho \in (0,\pi)$, let $S_\rho \in \mathcal{S}$ be the singly periodic Scherk

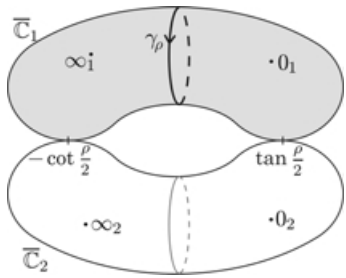

Figure 10 The Riemann surface $\mathbb{M}_\rho$ with nodes $\tan\frac{\rho}{2}, -\cot\frac{\rho}{2}$ and the embedded closed curve $\gamma_\rho \subset \bar{\mathbb{C}}_1$

surface of angle ρ. The limiting normal vectors of S_ρ at its nonhorizontal ends project stereographically to $\tan\frac{\rho}{2}$ and $-\cot\frac{\rho}{2}$. Recall that we can obtain two copies of S_ρ by taking limits from standard examples (see Section 2.2). We identify S_ρ with the list $(\mathbb{M}_\rho, g; 0_1, 0_2, \infty_1, \infty_2, [\gamma_\rho])$, where:

- $\mathbb{M}_\rho$ is a Riemann surface with nodes constructed by gluing two copies $\bar{\mathbb{C}}_1, \bar{\mathbb{C}}_2$ of $\bar{\mathbb{C}}$ with nodes $\tan\frac{\rho}{2}$ and $-\cot\frac{\rho}{2}$ (see Figure 10);
- $g\colon \mathbb{M}_\rho \to \bar{\mathbb{C}}$ is the map that associates to each point in $\mathbb{M}_\rho$ its complex value as a point in $\bar{\mathbb{C}}_j$, $j = 1, 2$ (in particular, the degree of g equals two);
- $0_j, \infty_j$ are respectively the zero and infinity in $\bar{\mathbb{C}}_j$, $j = 1, 2$; and
- $\gamma_\rho \subset \mathbb{C}_1$ is an embedded closed curve in the homology class $[\Gamma_1] + [\Gamma_2]$, where Γ_1 (resp. Γ_2) is a small loop in $\bar{\mathbb{C}}_1$ around 0_1 $\left(\text{resp. } \tan\frac{\rho}{2}\right)$ with the positive orientation.

Given this identification, we can see $\mathcal{S}$ in $\partial\mathcal{K} \subset \partial\mathcal{W}$. From Lemma 6 and Theorem 2 of [9], one deduces that $\tilde{\mathcal{W}} = \mathcal{W} \cup \mathcal{S}$ is a 4-dimensional complex manifold where L extends holomorphically, and this extended ligature map is a biholomorphism in a small neighborhood of $\mathcal{S}$ in $\tilde{\mathcal{W}}$. A straightforward computation gives us

$$L(S_\rho) = \left(2\csc\rho, -2\csc\rho, -2\pi i\tan\tfrac{\rho}{2}, 2\pi i\tan\tfrac{\rho}{2}\right). \tag{14}$$

3.2. The Classifying Map

In this section we study the topology of the space $\mathcal{K}$, and the key ingredient for this study will be the classifying map C that associates roughly to each marked standard surface its period at the ends and the horizontal component of its flux along a nontrivial homology class with zero period vector.

DEFINITION 3. Let $\tilde{\mathcal{K}} = \mathcal{K} \cup \mathcal{S}$ and define the *classifying map* $C\colon \tilde{\mathcal{K}} \to \mathbb{R}^+ \times \mathbb{C}$ by $C(M) = (a, b)$, where $a := \operatorname{Res}_{p_1}\frac{dh}{g}$ and $b := \int_\gamma g\, dh$ (hence $F_\gamma = (ib, 2\pi) \in \mathbb{C} \times \mathbb{R}$), provided that $M = (\mathbb{M}, g; p_1, p_2, q_1, q_2, [\gamma])$ and dh is the height differential of M.

Let $M = (\mathbb{M}, g;\, p_1, p_2, q_1, q_2, [\gamma])$ be a marked surface in $\tilde{\mathcal{K}}$ and let $C(M) = (a, b)$. Denote by γ_X a small loop around $X \in \mathbb{M}$, oriented positively. If $\tilde{M} = (\mathbb{M}, g;\, p_1, p_2, q_1, q_2, [\tilde{\gamma}])$ with $[\tilde{\gamma}] = [\gamma] + n([\gamma_{p_1}] + [\gamma_{q_1}]) + m([\gamma_{p_2}] + [\gamma_{q_2}])$, then $C(\tilde{M}) = (a, b + 2\pi a(n - m))$; see Lemma 3. Since we want to avoid associating more than one different image to the same geometrical surface, it is necessary to restrict

$$C\colon \tilde{\mathcal{K}} \to \Lambda = \{(a, b) \in \mathbb{R}^+ \times \mathbb{C} \mid 0 \leq \Re(b) < 2\pi a\} \equiv \mathbb{R}^+ \times \mathbb{S}^1 \times \mathbb{R}.$$

Recall that $\mathcal{K}$ is a 3-dimensional real analytic manifold (see Remark 3). It is clear from the foregoing definition that $C|_{\mathcal{K}}$ is smooth. Also note that C is essentially $L|_{\tilde{\mathcal{K}}}$. Since L extends as a biholomorphism in a small neighborhood of $\mathcal{S}$ in $\tilde{\mathcal{W}}$, it follows that $\tilde{\mathcal{K}}$ can be endowed with a structure of a 3-dimensional real analytic manifold and that $C\colon \tilde{\mathcal{K}} \to \Lambda$ is also smooth. Observe that $C|_{\mathcal{K}}$ is not proper, since $\mathcal{S}$ is contained in the boundary of $\mathcal{K}$ in $\tilde{\mathcal{W}}$ but $C(\mathcal{S}) \subset \Lambda$. More precisely, by (14) we have

$$C(S_\rho) = \left(2 \csc \rho, 2\pi i \tan \tfrac{\rho}{2}\right). \tag{15}$$

PROPOSITION 1. *The classifying map $C\colon \tilde{\mathcal{K}} \to \Lambda$ is proper.*

Proof. Take a sequence $\{M_n\}_n \subset \tilde{\mathcal{K}}$ such that $\{C(M_n) = (a_n, b_n)\}_n$ converges to some point $(a, b) \in \Lambda$. We shall prove that a subsequence of $\{M_n\}_n$ converges to a surface in $\tilde{\mathcal{K}}$.

First suppose that, after passing to a subsequence, $M_n \in \mathcal{K}$ for every n, and let $(\theta_n, \alpha_n, \beta_n) \in \mathcal{I}$ (see (11)) be the angles that determine the spherical configuration of $M_n = M_{\theta_n, \alpha_n, \beta_n}$. Extracting a subsequence, we can assume that $(\theta_n, \alpha_n, \beta_n) \to (\theta_\infty, \alpha_\infty, \beta_\infty) \in \left[0, \frac{\pi}{2}\right] \times \left[-\frac{\pi}{2}, \frac{\pi}{2}\right] \times [0, \pi]$. By equation (7) we deduce that $a(M_n)$ equals the modulus of $\mu(\theta_n) \sin\theta_n E(\theta_n, \alpha_n, \beta_n) \in \mathbb{C}$. As a result:

- If $\theta_\infty = \frac{\pi}{2}$, then $a(M_n) \to 0$. These limits correspond, after blowing up, to two vertical helicoids when $\alpha_\infty = 0$ and $\beta = \frac{\pi}{2}$ or else to two copies of a doubly periodic Scherk minimal surface (see Section 2.2).
- If $\theta_\infty \neq \frac{\pi}{2}$ but $\alpha_\infty = 0$ and $\beta_\infty \in \{\theta_\infty, \pi - \theta_\infty\}$, then $a(M_n) \to \infty$. These limits correspond to the vertical catenoid when $\theta_\infty = 0$ or else to a Riemann minimal example.

Therefore, the only possibilities are as follows.

- $\theta_\infty = 0$ and $(\alpha_\infty, \beta_\infty) \notin \{(0, 0), (0, \pi)\}$; then $\{M_n\}_n$ converges to two copies of a singly periodic Scherk minimal surface.
- $(\theta_\infty, \alpha_\infty, \beta_\infty) \in \mathcal{I}$, so $\{M_n\}_n$ converges to the standard example $M_{\theta_\infty, \alpha_\infty, \beta_\infty} \in \mathcal{K}$.
- $\alpha_\infty = \pm\frac{\pi}{2}$; hence $M_n \to M_{\theta_\infty, \pm\pi/2, \beta_\infty} = M_{\theta_\infty, \pi/2, 0}$ (see Remark 2).
- $\beta_\infty = \pi$; hence $M_n \to M_{\theta_\infty, \alpha_\infty, \pi} = M_{\theta_\infty, \alpha_\infty, 0}$.

Hence $\{M_n\}_n$ admits a subsequence converging in $\tilde{\mathcal{K}}$ (this can be also obtained by arguing as in the proof of [9, Thm. 5]).

Thus it suffices to prove that $C|_{\mathcal{S}}$ is proper, but this is clear by (15). This fact completes the proof of Proposition 1. □

4. The Classifying Map Is a Local Diffeomorphism

PROPOSITION 2. *The classifying map $C : \tilde{\mathcal{K}} \to \Lambda$ is a local diffeomorphism.*

Proof. The relationship between C and $L|_{\tilde{\mathcal{K}}}$ allows us to assure that C is a diffeomorphism in a small neighborhood of $\mathcal{S}$ in $\tilde{\mathcal{K}}$. Thus it only remains to demonstrate that $C|_{\mathcal{K}}$ is a local diffeomorphism. Consider a standard example $M \in \mathcal{K}$ and denote by $\tilde{M}$ its lifting to $\mathbb{R}^3$. It suffices to check that if $u\colon \tilde{M} \to \mathbb{R}$ is a Jacobi function that lies in the kernel of dC_M, then $u = 0$.

We can write $u = \langle \frac{d}{dt}\big|_0 \tilde{M}_t, N\rangle$ for certain variation $\{\tilde{M}_t\} \subset \mathcal{K}$ of $\tilde{M}_{t=0} = \tilde{M}$. Let $\mathcal{P}_t$ be the period lattice of $\tilde{M}_t \subset \mathbb{R}^3$, $M_t = \tilde{M}_t/\mathcal{P}_t$, and $(a_t, b_t) = C(M_t) \in \mathbb{R}^+ \times \mathbb{C}$. Since $u \in \ker(dC_M)$, it follows that

$$\tfrac{d}{dt}\big|_{t=0} a_t = 0 \quad \text{and} \quad \tfrac{d}{dt}\big|_{t=0} b_t = 0. \tag{16}$$

By Lemma 2 and after normalizations, the conjugation map $*\colon \mathcal{K} \to \mathcal{K}$, which associates to each standard example its conjugate surface, is a well-defined map. Furthermore, $*$ is clearly differentiable because it is the restriction to $\mathcal{K}$ of the map $(g, \phi) \to (g, i\phi)$ on the space of allowed Weierstrass data. Since clearly $* \circ * =$ identity, we may deduce that $*$ is a diffeomorphism. Hence it suffices to prove that the tangent vector v defined as the image of u by the differential of $*$ vanishes identically. Notice that $v = \langle \frac{d}{dt}\big|_{t=0} \tilde{M}_t^*, N\rangle$, where $\tilde{M}_t^*$ is the conjugate surface of $\tilde{M}_t$. In particular, v is a Jacobi function on $\tilde{M}^*$, which is moreover bounded because all the $\tilde{M}_t^*$ have horizontal ends.

First suppose that v is a bounded Jacobi function on the quotient M^* of $\tilde{M}^*$ by its period lattice. By Remark 3 we know that v is of the kind $v = \langle N, V\rangle$ for some $V \in \mathbb{R}^3$. Theorem 3 in [8] assures that there exists a unique element X_v of the space of complete branched minimal immersions into $\mathbb{R}^3$ (including the constant maps) with finite total curvature and planar ends whose extended Gauss map is N and such that $\langle X_v, N\rangle = v$. Thus X_v is constantly V, and v corresponds to a translation of $\tilde{M}^*$ in $\mathbb{R}^3$. Because we are considering the surfaces in $\mathcal{K}$ up to translations, it follows that $v = 0$. Hence we have only to prove that v descends to the quotient M^*.

Recall that the flux of $\tilde{M}_t$ at its ends is (up to sign) $H_t = (\pi a_t, 0, 0)$ and that its flux along the homology class in the last component (viewed as a marked standard example) is $T_t = (ib_t, 2\pi) \in \mathbb{C} \times \mathbb{R} \equiv \mathbb{R}^3$. Therefore, the period lattice of $\tilde{M}_t^*$ (before normalization) is generated by H_t and T_t. We parameterize $\tilde{M}_t^*$ by $\psi_t^*\colon \tilde{M} \to \tilde{M}_t^*$ and we denote by $S_{1,t}, S_{2,t}\colon \tilde{M} \to \tilde{M}$ the diffeomorphisms induced by H_t, T_t—that is, those satisfying

$$\psi_t^* \circ S_{1,t} = \psi_t^* + H_t \quad \text{and} \quad \psi_t^* \circ S_{2,t} = \psi_t^* + T_t. \tag{17}$$

By (16), $\frac{d}{dt}\big|_{t=0} H_t = \frac{d}{dt}\big|_{t=0} T_t = \vec{0}$. Therefore,

$$\begin{aligned} v \circ S_{1,0} &= \langle \tfrac{d}{dt}\big|_{t=0} \psi_t^*, N\rangle \circ S_{1,0} = \langle \tfrac{d}{dt}\big|_{t=0} (\psi_t^* \circ S_{1,t}), N\rangle \\ &\overset{(17)}{=} \langle \tfrac{d}{dt}\big|_{t=0} \psi_t^*, N\rangle + \langle \tfrac{d}{dt}\big|_{t=0} H_t, N\rangle = v. \end{aligned}$$

Analogously, $v \circ S_{2,0} = v$. Thus v descends to the quotient and Proposition 2 is proved. □

5. The Topology of $\mathcal{K}$ (Proof of Theorem 3)

By Propositions 1 and 2, $C\colon \tilde{\mathcal{K}} \to \Lambda$ is a proper local diffeomorphism and so is a finite sheeted covering map. We deduce from Lemma 1, Remark 2, and equation (15) that the only surfaces $M \in \tilde{\mathcal{K}}$ with $C(M) = (a, 0)$, for some $a > 0$, are the standard examples $M_{\theta,0,0}$. Since $a(M_{\theta,0,0}) = \mu(\theta)$ is a strictly decreasing function in θ, the number of sheets of the covering map C is one; hence it is a diffeomorphism. Moreover, the set $C(\mathcal{S})$ consists of the proper arc $\rho \in (0, \pi) \mapsto \left(2\csc\rho, 2\pi i \tan\frac{\rho}{2}\right)$, whereby we deduce that $\mathcal{K}$ is diffeomorphic to the complement in Λ of such an arc, which in turn is diffeomorphic to $\mathbb{R} \times (\mathbb{R}^2 - \{(\pm 1, 0)\})$. This proves Theorem 3.

REMARK 4. Since $C\colon \mathcal{K} \to C(\mathcal{K}) \equiv \mathbb{R} \times (\mathbb{R}^2 - \{(\pm 1, 0)\})$ is a diffeomorphism, any standard example is completely determined by its image through C. This justifies the words *classifying map* for C.

Recall that we can identify some standard examples in $\mathcal{K}$ by symmetries (see Remark 2). Since there are standard examples invariant by such symmetries, we deduce that the quotient of $\mathcal{K}$ by these symmetries has the structure of a 3-dimensional orbifold. Notice that this quotient space is the moduli space of doubly periodic minimal surfaces with parallel ends and genus 1 in the quotient.

References

[1] L. Hauswirth and M. Traizet, *The space of embedded doubly-periodic minimal surfaces,* Indiana Univ. Math. J. 51 (2002), 1041–1079.

[2] D. Hoffman and W. H. Meeks III, *The strong halfspace theorem for minimal surfaces,* Invent. Math. 101 (1990), 373–377.

[3] H. Karcher, *Embedded minimal surfaces derived from Scherk's examples,* Manuscripta Math. 62 (1988), 83–114.

[4] ———, *Construction of minimal surfaces,* Surveys in Geometry, pp. 1–96, Univ. of Tokyo, 1989, and Lecture Notes no. 12, SFB256, Bonn, 1989.

[5] H. Lazard-Holly and W. H. Meeks III, *Classification of doubly-periodic minimal surfaces of genus zero,* Invent. Math. 143 (2001), 1–27.

[6] W. H. Meeks III, J. Pérez, and A. Ros, *Uniqueness of the Riemann minimal examples,* Invent. Math. 133 (1998), 107–132.

[7] W. H. Meeks III and H. Rosenberg, *The global theory of doubly periodic minimal surfaces,* Invent. Math. 97 (1989), 351–379.

[8] S. Montiel and A. Ros, *Schrödinger operators associated to a holomorphic map,* Global differential geometry and global analysis (Berlin, 1990), Lecture Notes in Math., 1481, pp. 147–174, Springer-Verlag, Berlin, 1991.

[9] J. Pérez, M. M. Rodríguez, and M. Traizet, *The classification of doubly periodic minimal tori with parallel ends,* J. Differential Geom. 69 (2005), 523–577.
[10] H. F. Scherk, *Bemerkungen über die kleinste Fläche innerhalb gegebener Grenzen,* J. Reine Angew. Math. 13 (1835), 185–208.

Departamento de Geometría y Topología
Universidad de Granada
Granada, E-18071
Spain

magdarp@ugr.es